Internal Heat Generation/Absorption Effects on MHD Radiative Flow Over a Non-Isothermal Stretching/Shrinking Surface Embedded in a Porous Medium

J. Wilfred Samuel Raj[11] and S.P. Anjali Devi[2]

[1]*Department of Mathematics, The American College, Madurai, Tamilnadu, India.*
[2]*Department of Applied Mathematics, Bharathiar University, Coimbatore, Tamilnadu, India.*

ABSTRACT

A comprehensive study has been made to investigate the effects of thermal radiation and internal heat generation/absorption on nonlinear hydromagnetic flow and heat transfer over a stretching/shrinking surface with variable surface temperature embedded in a porous medium. Using the similarity transformations, the governing equations are transformed into nonlinear ordinary differential equations. Then the numerical solution of the nonlinear boundary value problem is found using Nachtsheim Swigert shooting iteration scheme for the satisfaction of asymptotic boundary conditions along with Fourth Order Runge Kutta method. The effects of different physical parameters governing the flow and heat transfer characteristics such as magnetic parameter, suction parameter, stretching/shrinking parameter, permeability parameter, prandtl number, heat generation/absorption parameter, radiation parameter and w all temperature parameter are discussed. Favourable comparisons of present numerical result with previous published work on various special cases of the problem are obtained. Numerical solutions obtained are also validated by comparing with the closed form solutions.

Keywords: Boundary Layer, Heat Transfer, Internal Heat Generation/Absorption, MHD, Stretching/ Shrinking Surface and Thermal Radiation.

1. INTRODUCTION

Flow and heat transfer aspects of a continuously moving surface is of considerable interest in many industrial applications such as metal extrusion, glass production, hot rolling, continuous casting, manufacturing of plastic and rubber sheets and crystal growing. The pioneering work was carried out by Sakiadis. Sakiadis [1, 2] analyzed the boundary layer assumptions and boundary layer flow on a continuously stretching sheet with constant speed. Many authors have reported flow and heat transfer by considering various physical situations. Crane [3] initiated the flow past a stretching plate. Chakrabarti and Gupta [4] reported hydromagnetic flow and heat transfer over a stretching sheet. Non-Newtonian flow past a stretching sheet was studied by Siddappa and Subhash [5]. The flow and heat transfer of a viscoelastic fluid over a stretching sheet has been explored by Danpat *et al.* [6]. Radiation effect on heat transfer over a stretching surface was examined by Elbashbeshy [7]. Liao [8] analyzed a new branch of solution of boundary layer flows over a stretching flat plate. Ishak *et al.* [9] presented hydromagnetic flow and heat transfer adjacent to stretching vertical sheet. Prasad *et al.* [10] considered mixed convection heat transfer over a nonlinear stretching surface with variable fluid properties. Anjali devi *et al.* [11] analyzed the radiation effects on MHD boundary layer flow and heat transfer over a nonlinear stretching surface with variable wall temperature in the presence of non-uniform heat source/sink.

Shrinking sheet is a surface which decreases in size to a certain area due to an imposed suction or external heat. For this flow configuration, the sheet is shrunk towards a slot. It is also shown that the mass suction is needed generally to maintain the flow over a shrinking surface. The investigation of flow over a shrinking sheet has lot of application in industries. One of the most common applications of shrinking sheet problems in industries is shrinking film. The applications of shrinking surface motivated the investigators to deal with the problems of flow over a shrinking surface. The existence and uniqueness of the solution of viscous flow over a shrinking sheet was determined by Micklavcic and Wang [12]. Boundary layer flow over a shrinking sheet with power law velocity was explored by Fang [13]. Yao and Chen [14] obtained a new analytical solution branch for the Blasius equation with a shrinking sheet. Thermal boundary layer flow over a shrinking sheet was investigated by Fang and Zhang [15]. Boundary layer flow and heat transfer over an exponentially shrinking vertical sheet with suction was addressed by Rohini *et al.* [16]. Flow over shrinking sheet under different physical aspects have been discussed in the literature [17- 25].

A new dimension has been made to study the viscous, electrically conducting fluid flow over stretching/shrinking surface, which is the consideration of effects of thermal radiation and internal heat generation/absorption. Thermal radiation effects play a significant role in controlling heat transfer in polymer industry where the quality of the final product depends on the heat controlling factors to some extent. Recently, Krishnendu Bhattacharyya and Layek [26] studied the effect of suction/blowing on steady boundary layer stagnation point flow and heat transfer towards a shrinking sheet with thermal radiation. To the best of our knowledge, there are only few published papers on viscous flow and heat transfer due to a shrinking surface with radiation and internal heat generation/absorption effects [27-30], wherein the effect of internal heat generation/absorption on heat transfer of a radiating fluid through a porous medium over a stretching/shrinking surface with variable temperature were not considered.

The objective of the present study is two fold: first to include the effects of thermal radiation and internal heat generation/absorption in heat transfer equation, secondly to carry out heat transfer analysis, when the surface embedded in a porous medium is prescribed with variable temperature. The numerical results of the flow and heat transfer characteristics are presented graphically.

2. MATHEMATICAL FORMULATION

2.1 Flow Analysis

Consider a steady, nonlinear, laminar, two-dimensional boundary layer forced convective flow of a viscous, incompressible, electrically conducting and radiating fluid over a continuous stretching/shrinking surface coinciding with the plane $y = 0$ and is embedded in a porous medium where the flow being confined to $y > 0$.
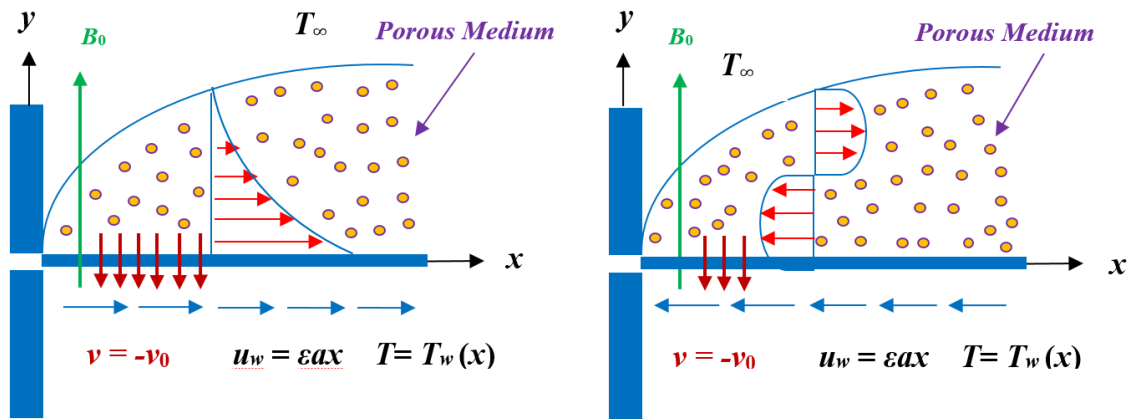
Figure 1. (a) Stretching Surface ($\varepsilon > 0$)   (b) Shrinking Surface ($\varepsilon < 0$)

The fluid is considered to be grey, absorbing and emitting but non-scattering medium. The x-coordinate is measured along the stretching/shrinking surface and y coordinate is measured perpendicular to it in the outward direction. The fluid properties are assumed to be constant. A magnetic field B_0 of uniform strength is applied transversely to the direction of the flow. The magnetic Reynolds number of the flow is taken to be sufficiently small enough, so that the induced magnetic field can be neglected in comparison with the applied magnetic field so that $\boldsymbol{B} = B_0\,\hat{\jmath}$. Since the flow is steady $curl\,\boldsymbol{E} = 0$. Also $div\,\boldsymbol{E} = 0$ in the absence of surface charge density and hence $\boldsymbol{E} = 0$ is assumed. The viscous and Joule's dissipation terms in the energy equation are neglected.

Within the framework and the above assumptions, the boundary layer equations of mass and momentum can be described by the following conservation equations

$$\frac{\partial u}{\partial x} + \frac{\partial v}{\partial y} = 0 \tag{1}$$

$$u\frac{\partial u}{\partial x} + v\frac{\partial u}{\partial y} = \nu\frac{\partial^2 u}{\partial y^2} - \frac{\sigma B_0^2}{\rho}u - \frac{\nu}{k_p}u \tag{2}$$

Here, u and v denotes the fluid velocity respectively in the x and y directions, ν is the kinematic viscosity, σ is electrical conductivity of the fluid, B_0 is the applied magnetic field, ρ is the density of the fluid and k_p is the permeability of the medium.

The boundary conditions corresponding to the continuity and momentum equations are given below

$$u = \varepsilon\, u_w, \qquad v = -v_0 \qquad \text{at } y = 0 \quad , \qquad\qquad u \to 0 \qquad \text{as } y \to \infty \tag{3}$$

where ε is the stretching/shrinking parameter with $\varepsilon > 0$ for stretching and $\varepsilon < 0$ for shrinking, $u_w = a\,x$ is the stretching/shrinking surface velocity, $a > 0$ is a dimensional constant, $v_0 > 0$ is the constant suction velocity. The equation of continuity is satisfied if a stream function ψ is chosen such that $u = \dfrac{\partial \psi}{\partial y}, \quad v = \dfrac{\partial \psi}{\partial x}$

The following similarity transformations are introduced

$$\eta = y\left(\frac{a}{\nu}\right)^{\frac{1}{2}}, \; \psi(x,y) = \sqrt{a\nu}\, x\, F(\eta) \tag{4}$$

Equations (1) and (2) admit self similar solution of the form

$$u = a x F'(\eta), \quad v = \sqrt{a v}\, F(\eta) \tag{5}$$

Substituting equations (4) and (5), the momentum equation (2) and its boundary conditions in (3) become,

$$F''' + F F'' - (F')^2 - (M^2 + \lambda^{-1}) F' = 0 \tag{6}$$

with its boundary conditions $F(0) = S$, $F'(0) = \varepsilon$ and $F'(\infty) = 0$ (7)

where, the prime denotes differentiation with respect to η, $M^2 = \dfrac{\sigma B_0^2}{\rho a}$ is the Magnetic

parameter, $\lambda = \dfrac{k_p a}{v}$ is the Permeability parameter, $S = \dfrac{v_0}{\sqrt{a v}}$ is the Suction parameter.

2.1.1 Skin friction coefficient

The parameter of engineering interest is the skin friction coefficient. The skin friction coefficient

is determined from $C_f = \dfrac{\tau_w}{\rho u_w^2 / 2}$ (8)

where $\tau_w = \mu \left(\dfrac{\partial u}{\partial y} \right)_{y=0}$ is the wall shearing stress on the surface of the shrinking sheet and μ is

the coefficient of viscosity. The expression for skin friction coefficient is given by $\sqrt{Re_x}\, \dfrac{C_f}{2} = F''(0)$

where $Re_x = \dfrac{a x^2}{v}$ is the local Reynolds number.

2.2 Heat Transfer Analysis

The energy equation includes the effect of radiation and heat generation/absorption. It is assumed that the radiative heat flux in the x-axis is negligible in comparison to that in the y-axis. Further, it is assumed that the temperature of the surface $T_w(x)$ varies as $T_w(x) = T_\infty + A x^r$ where A is a constant which depends on thermal properties of the fluid, T_∞ is the temperature far away from the sheet and r is the wall temperature parameter. Considering the above mentioned effects and assumptions, the boundary layer energy equation is given by

$$\rho C_p \left(u \frac{\partial T}{\partial x} + v \frac{\partial T}{\partial y} \right) = k \frac{\partial^2 T}{\partial y^2} - \frac{\partial q_r}{\partial y} + Q(T - T_\infty) \tag{9}$$

where C_p is the specific heat at constant pressure, T is the fluid temperature, k is the thermal conductivity of the fluid, q_r is the radiative heat flux, $Q > 0$ is the volumetric rate of heat generation and $Q < 0$ is the volumetric rate of heat absorption.

The Rosseland approximation (Brewster [31]) is used to simplify the radiative heat flux in the

energy equation which gives $q_r = -\dfrac{4\sigma^*}{3k^*} \dfrac{\partial T^4}{\partial y}$ (10)

Here σ^* and k^* denotes the Stefan-Boltzmann constant and mean absorption coefficient respectively. Assuming that the temperature variation within the flow is such that T^4 can be

expanded in a Taylor series about T_∞ (Raptis *et al.* [32]) as $T^4 = T_\infty^4 + 4T_\infty^3(T - T_\infty) + 6T_\infty^2(T - T_\infty)^2 + \ldots$ and neglecting the higher order terms beyond the first degree in $(T - T_\infty)$, T^4 can be given as

$$T^4 \cong 4T_\infty^3 T - 3T_\infty^4 \tag{11}$$

Substituting equations (10) and (11), energy equation takes the form

$$\rho C_p \left(u\frac{\partial T}{\partial x} + v\frac{\partial T}{\partial y} \right) = k\frac{\partial^2 T}{\partial y^2} + \frac{16\sigma^* T_\infty^3}{3k^*}\frac{\partial^2 T}{\partial y^2} + Q(T - T_\infty) \tag{12}$$

with its corresponding boundary conditions,

$$T = T_w(x) = T_\infty + Ax^r \quad \text{at} \quad y = 0, \qquad\qquad T \to T_\infty \quad \text{as } y \to \infty \tag{13}$$

The dimensionless temperature θ is defined as $\theta(\eta) = \dfrac{T - T_\infty}{T_w(x) - T_\infty}$. Using the dimensionless temperature $\theta(\eta)$ and the velocities u and v as given in equation (5), the energy equation in non-dimensional form is obtained as

$$\left(\frac{3Rd + 4}{3Rd\,\text{Pr}}\right)\theta'' + F\theta' - (rF' - Hs)\theta = 0 \tag{14}$$

where $\text{Pr} = \dfrac{\mu C_p}{k}$ is the Prandtl number, $Hs = \dfrac{Q}{a\rho C_p}$ is the Heat generation/absorption parameter and $Rd = \dfrac{kk^*}{4\sigma^* T_\infty^3}$ is the Radiation parameter.

The boundary conditions in (13) take the nondimensional form as

$$\theta(\eta) = 1 \quad \text{at } \eta = 0 \quad \text{and} \qquad \theta(\eta) \to 0 \quad \text{as } \eta \to \infty \tag{15}$$

2.2.1 Non-Dimensional Rate of Heat Transfer

The dimensionless rate of heat transfer (Local Nusselt number) from the shrinking surface is derived from $Nu_x = \dfrac{xq_w}{k(T_w - T_\infty)}$
$$\tag{16}$$

where $q_w = \left(-k\dfrac{\partial T}{\partial y} + q_r\right)_{y=0}$ is the net heat flux at the wall. The local Nusselt number is obtained in terms of the dimensionless temperature at the sheet surface as

$$\frac{Nu_x}{\sqrt{\text{Re}_x}} = -\left(1 + \frac{4}{3Rd}\right)\theta'(0)$$

3. NUMERICAL SIMULATION

The nonlinear differential equations (6) and (14), along with the boundary conditions (7) and (15) are solved numerically by converting the boundary value problem into an initial value problem, using the most efficient Nachtsheim Swigert shooting iteration scheme along with

Fourth Order Runge Kutta algorithm. To solve the boundary value problem constituting (6) and (14), the values of $F''(0)$ and $\theta'(0)$ are needed. The initial guess values for $F''(0)$ and $\theta'(0)$ are chosen and the Nachtsheim Swigert shooting iteration scheme for satisfaction of asymptotic boundary conditions is applied to obtain the values of $F''(0)$ and $\theta'(0)$. The process is repeated until the results are corrected up to the desired accuracy of 10^{-5} level, which fulfils the convergence criterion. Later, the numerical solutions are obtained utilizing Fourth Order Runge Kutta method. The convergence criterion largely depends on fairly good guesses of initial conditions in the shooting technique. Numerical results are obtained and presented for various values of physical parameters like Magnetic parameter, Suction parameter, Shrinking/Stretching parameter, Prandtl number, Heat generation/absorption parameter, Radiation parameter and Wall temperature parameter.

4. CLOSED FORM SOLUTION

The closed form solution is obtained for Momentum and Energy equations in case of shrinking surface i.e. ε =-1.

4.1 Momentum Equation

The equation (6) with its boundary condition in (7) admits the solution of the form (Following Chakrabarti and Gupta [4]):

$$F(\eta)=S-\frac{1}{\alpha}(1-e^{-\alpha\eta}) \text{ and } F'(\eta)=-e^{-\alpha\eta} \tag{17}$$

Where $\alpha=\dfrac{S+\sqrt{S^2+4(M^2-1+\lambda^{-1})}}{2}$. In the absence of porous medium the analytical solution of $F(\eta)$ is same as that of Fang and Zhang [15].

4.2 Energy Equation

To obtain the solution of the energy equation (14), we introduce a new variable

$$\xi=\frac{P}{\alpha^2}e^{-\alpha\eta} \tag{18}$$

Using the new independent variable defined in (18) we get the homogeneous confluent hypergeometric equation as

$$\xi\ddot{\theta}+(1-a_0-\xi)\dot{\theta}+\left(r+\frac{P\,Hs}{\alpha^2\,\xi}\right)\theta=0 \tag{19}$$

where $a_0=\dfrac{P}{\alpha^2}(\alpha^2-M^2-\lambda^{-1})$, $P=\frac{3\,Rd\,Pr}{3\,Rd\,+\,4}$ and the dot denotes the differentiation with respect to ξ.

Subsequently, the corresponding boundary conditions (13) take the form

$$\theta\left(\xi=\frac{P}{\alpha^2}\right)=1 \text{ and } \theta(\xi=0)=0 \tag{20}$$

The solution of (19) may be expressed as follows

$$\theta(\xi)=\frac{\xi^{\frac{a_0+b_0}{2}}\Phi\left(\frac{a_0+b_0-2r}{2},1+b_0;\xi\right)}{\left(\frac{P}{\alpha^2}\right)^{\frac{a_0+b_0}{2}}\Phi\left(\frac{a_0+b_0-2r}{2},1+b_0;\frac{P}{\alpha^2}\right)} \qquad (21)$$

where $\Phi(a,b;x)$ is the confluent hypergeometric function of first kind and $b_0=\sqrt{a_0^2-\frac{4\,P\,Hs}{\alpha^2}}$.

Expression for θ in terms of similarity variable η can be expressed as

$$\theta(\eta)=e^{-\alpha\left(\frac{a_0+b_0}{2}\right)\eta}\frac{\Phi\left(\frac{a_0+b_0-2r}{2},1+b_0;\frac{P}{\alpha^2}e^{-\alpha\eta}\right)}{\Phi\left(\frac{a_0+b_0-2r}{2},1+b_0;\frac{P}{\alpha^2}\right)} \qquad (22)$$

5. RESULTS AND DISCUSSION

A mathematical modelling of steady, two-dimensional, nonlinear, hydromagnetic boundary layer flow over a stretching/shrinking surface with variable temperature embedded in a porous medium in the presence of radiation and internal heat generation/absorption is carried out. Numerical solution of the problem is obtained utilizing the efficient shooting method along with Nachtsheim Swigert iteration scheme to satisfy the asymptotic boundary conditions. Numerical solutions have been carried out to analyze the influence of physical parameters that arise in the study namely Magnetic parameter, Suction parameter, Permeability parameter, Stretching/Shrinking parameter Prandtl number, Heat generation/absorption parameter, Radiation parameter and Wall temperature parameter.

Table 1 represents the comparison of skin friction coefficient for different values of *S* in the present study with the results of Muhaimin *et al.* [33] and Bhattacharyya [23]. In the case of two-dimensional flow the results reduce to that of Muhaimin *et al.* [33]. It is also seen that in the absence of porous medium, the results for skin friction coefficient agree well with the results of Bhattacharyya [23].

Table 2 depicts the skin friction coefficient for various values of Suction parameter, Magnetic parameter and Shrinking/Stretching parameter. The table values show that the skin friction coefficient increases due to the increasing effect of Suction, Magnetic whereas it decreases with an increase in Stretching/Shrinking parameter.

Table 3 shows the variation in non-dimensional rate of heat transfer for various values of the physical parameters involved in the study. It is clear that the effect of Suction parameter, Magnetic parameter, Stretching/Shrinking parameter, Prandtl number and Radiation parameter is to enhance the dimensionless rate of heat transfer while the effect of Heat generation parameter and Wall temperature parameter is to reduce the dimensionless rate of heat transfer for its increasing values.

Table 4 depicts the comparison of the present numerical results with the analytical results for the case of shrinking surface. The validity of the present numerical results along with the accuracy of the numerical technique is evident from the table.

Table 1 Comparison of results for skin friction coefficient $F''(0)$ when $M^2 = 2.0$, $\varepsilon = -1$

S	Present study	Muhaimin *et al.* [33]	Bhattacharyya [23]
2.0	2.414214	2.414214	2.414300
3.0	3.302775	3.302775	3.302750
4.0	4.236068	4.236068	4.236099

Table 2 Skin friction coefficient for different S, M^2 and ε when $S = 2.5$, $M^2 = 1$, $\varepsilon = -1$, $\lambda = 10$

S	M^2	ε	$F''(0)$
2.0			2.048808
2.5			2.539380
3.0	1.0	-1.0	3.032971
3.5			3.528342
4.0			4.024846
	0.0		2.063941
	1.0		2.539380
2.5	3.0	-1.0	3.163766
	5.0		3.629601
	7.0		4.018121
		-1.0	2.539800
2.5	1.0	-0.5	1.360272
		0.5	-1.514171
		1.0	-3.163766

Figures 2 and 3 display the comparison of the results of $F'(\eta)$ and $\theta(\eta)$ for various values of S in the absence of porous medium ($\lambda = 10^9$), radiation effects ($Rd = 10^9$) and for the case of constant surface temperature ($r = 0$). The figures show that the results are in good agreement with that of Bhattacharyya [23], which guarantees the numerical scheme applied.

Figure 4 elucidates the effect of Magnetic parameter over the dimensionless velocity. Due to the presence of transverse magnetic field the velocity gets accelerated. This happens due to the force arising from the interaction of magnetic and electric fields during the motion of the electrically conducting fluid. The momentum boundary layer thickness is reduced due to enhancing values of Magnetic parameter.

The effect of Suction parameter on flow field when the Magnetic parameter is fixed is shown in Figure 5. It is observed that the wall suction has the tendency to reduce the momentum boundary layer thickness. Further it is noted that a steady raise in the velocity accompanies a rise in Suction parameter, with all profiles tending asymptotically to horizontal axis.

Figure 6 demonstrates the effect of Stretching/Shrinking parameter on the velocity distribution. It is found that the effect of Stretching/ Shrinking parameter is to accelerate the dimensionless

velocity. Variation in skin friction coefficient against Permeability parameter for different values of Magnetic parameter is demonstrated in Figure 7. The influence of Magnetic parameter over skin friction coefficient is to elevate it. Figure 8 presents the skin friction coefficient against Permeability parameter for various values of Suction parameter. It is evident that the skin friction coefficient enhances due to raise in Suction parameter.

The impact of Magnetic parameter over the non-dimensional temperature is portrayed in Figure 9. It is clear from the figure that there is a fall in temperature accompanied with an increase in Magnetic parameter. Figure 10 exhibits the effect of Suction parameter over the temperature distribution. It is vivid that the porosity in the plate reduces the thermal boundary layer thickness, which causes a drop in the temperature of the fluid. Dimensionless temperature profiles for various values of Stretching/Shrinking parameter are depicted in Figure11. It is observed that an increase in Stretching/Shrinking parameter leads to thinning of boundary layer thickness.

Table 3 Non-dimensional rate of heat transfer when $S = 2.5$, $M^2 = 1$, $\varepsilon = -1$, $\lambda = 10$, $Pr = 0.71$, $Rd = 2$, $Hs = 0.1$ and $r = 2$

S	M^2	ε	Pr	Hs	Rd	r	$-\left(1+\dfrac{4}{3Rd}\right)\theta'(0)$
2.0	1.0	-1.0	0.71	0.1	2.0	2.0	0.408986
2.5							1.032182
3.0							1.534184
3.5							1.984970
4.0							2.408148
2.5	0.0	-1.0	0.71	0.1	2.0	2.0	0.895610
	1.0						1.032182
	3.0						1.150116
	5.0						1.212935
	7.0						1.254921
2.5	1.0	-1.0	0.71	0.1	2.0	2.0	1.032182
		-0.5					1.402114
		0.5					1.966738
		1.0					2.198212
2.5	1.0	-1.0	0.71	0.1	2.0	2.0	1.032182
			1.00				1.578380
			1.50				2.594268
			2.30				4.347326
			7.00				15.64727
2.5	1.0		0.71	0.00	2.0	2.0	1.132497
				0.10			1.032182
				0.20			0.915810
				0.30			0.772963
				0.35			0.684104
2.5	1.0		0.71	0.1	1.0	2.0	0.944425
					2.0		1.032182
					3.0		1.069005
					5.0		1.102951
					10^9		1.164827

2.5	1.0	0.71	0.1	2.0	0.0	1.484084
					1.0	1.263369
					2.0	1.032182
					3.0	0.789452
					4.0	0.533951
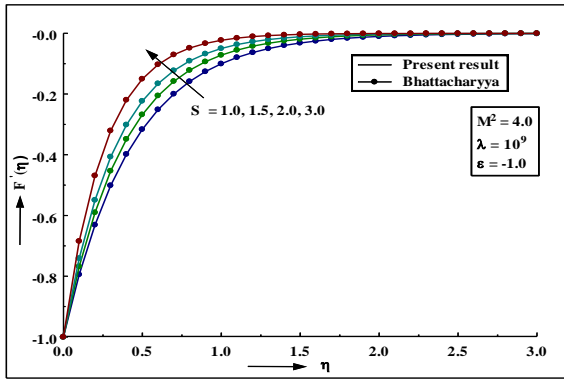
Figure 2. Comparison graph showing dimensionless velocity for various *S.*
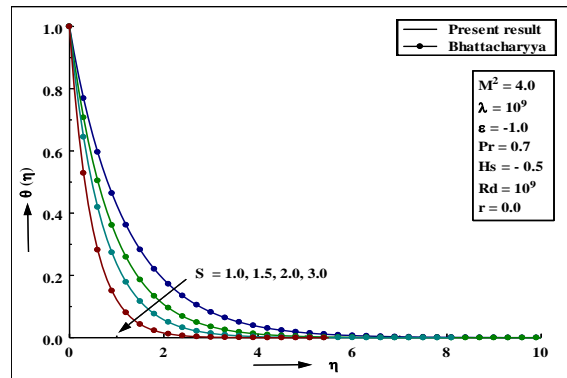
Figure 3. Comparison graph showing dimensionless temperature for various *S.*
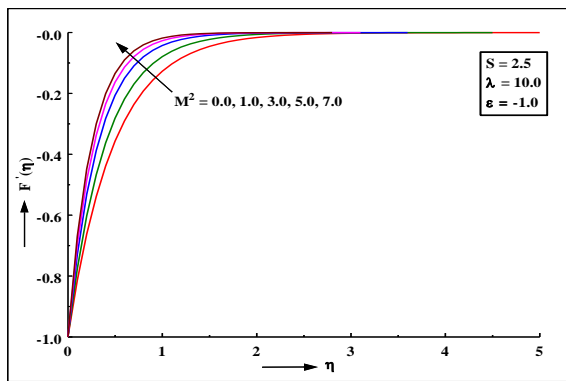
Figure 4. Dimensionless velocity profiles for various M^2.
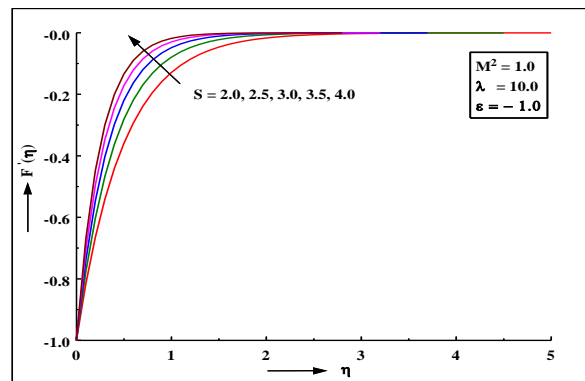
Figure 5. Dimensionless velocity profiles for various *S.*
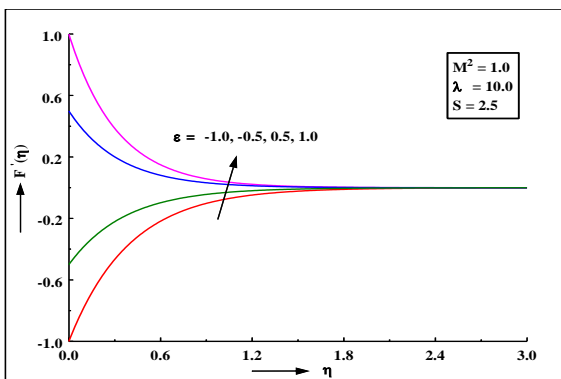
Figure 6. Dimensionless velocity profiles for various *ε.*
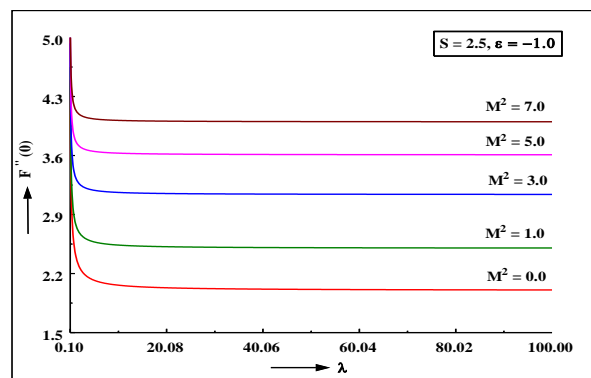
Figure 7. Skin friction coefficient for various M^2.

Figure 13 reveals the variation in temperature distribution within the boundary layer for various values of Heat generation parameter. The temperature of the fluid rises for higher values of Heat generation parameter. It is also noted that the thermal boundary layer thickness becomes thicker due to increase in Heat generation parameter. This is due to the fact that the thermal boundary layer generates energy which causes the temperature rise considerably with an increase in value of Heat generation parameter. Figure 14 shows the variation in temperature distribution for various values of Heat absorption parameter. The temperature of the fluid decreases for higher values of Heat absorption parameter. The thermal boundary layer thickness reduces due to increase in Heat absorption parameter.
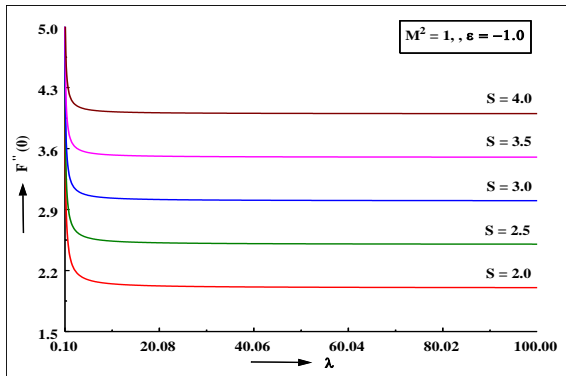
Figure 8. Skin friction coefficient for various *S.*
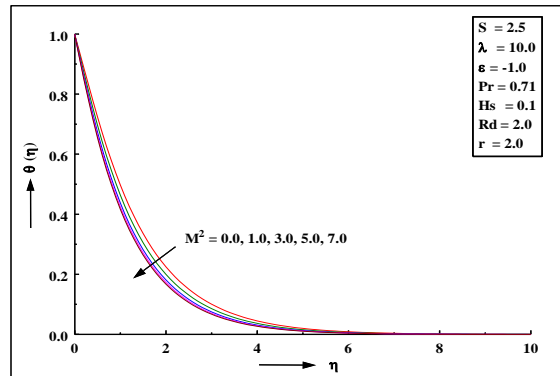
Figure 9. Dimensionless temperature profiles for various M^2.
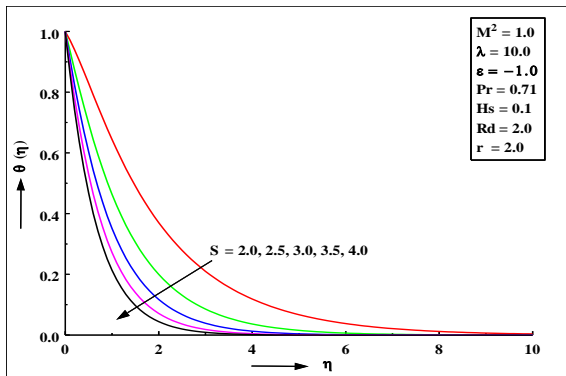
Figure 10. Dimensionless temperature profiles for various *S.*
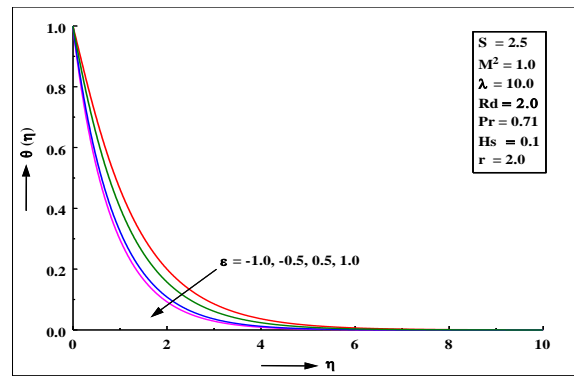
Figure 11. Dimensionless temperature profiles for various ε.
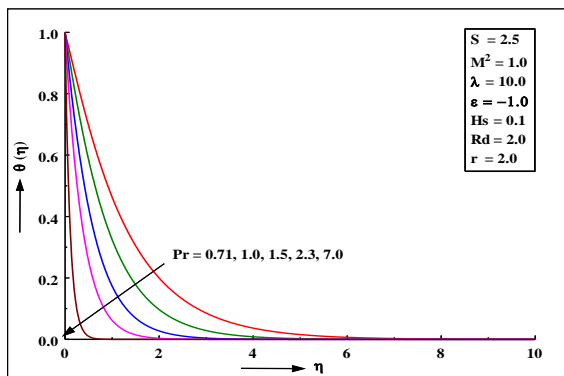
Figure 12. Dimensionless temperature profiles for various *Pr.*
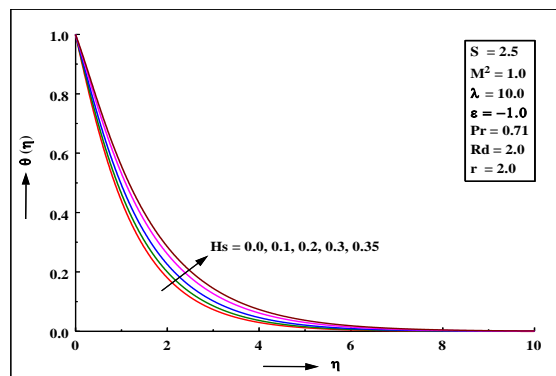
Figure 13. Dimensionless temperature profiles for various *Hs.*

49

Figure 15 illustrates the typical temperature profiles for various values of the Radiation parameter. The effect of radiation becomes more significant as $Rd \to 0$ ($Rd \neq 0$) and can be neglected when $Rd \to \infty$. The effect of radiation parameter is to reduce the temperature significantly in the flow region. By increasing the values of Radiation parameter, the fluid temperature decreases accompanied with a decrease in the thermal boundary layer thickness. This result can be explained by a fact that an increase in radiation parameter means the release of heat energy from the flow region which causes reduction in fluid temperature decreases as the thermal boundary layer thickness becomes thinner.

The temperature of the fluid for different values of Wall temperature parameter when all other parameters are kept constant is presented in Figure 16. It is evident from the graph that the increasing effect of wall temperature parameter gives rise to enhancement in temperature significantly.
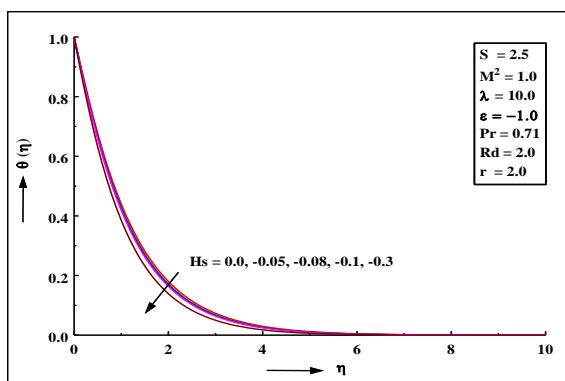
Figure 14. Dimensionless temperature profiles for various *Hs.*
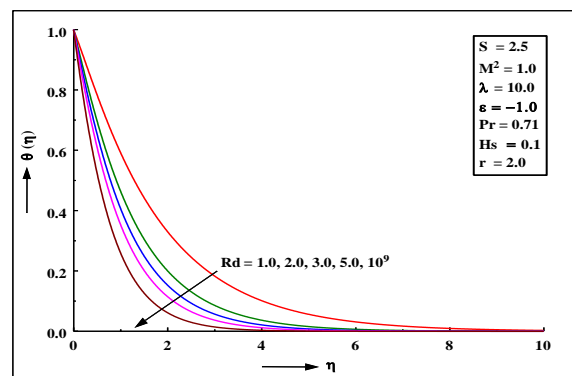
Figure 15. Dimensionless temperature profiles for various *Rd.*
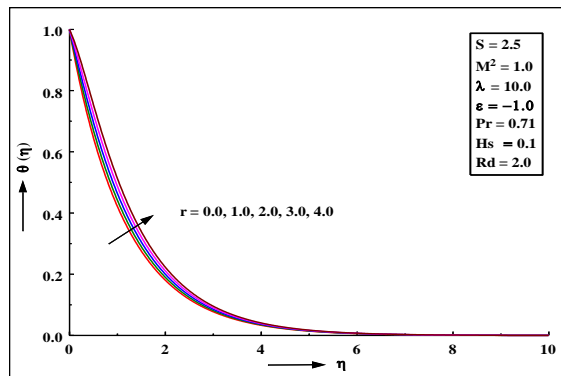
Figure 16. Dimensionless temperature profiles for various *r.*

6. CONCLUSION

In this paper, the effects of radiation and internal heat generation/absorption on nonlinear hydromagnetic boundary layer flow and heat transfer over a stretching/shrinking surface embedded in a porous medium have been investigated. The numerical results obtained have been validated by comparing it with the available results of shrinking sheet problems under some limiting cases. In the absence of porous medium, radiation effects and in the case of constant surface temperature, the results are in good agreement with that of Bhattacharyya [23]. The inclusion of Radiation and Heat generation/absorption effects has tremendous change on heat transfer characteristic.

The following main conclusion can be drawn from the present study:

- The effect of Radiation parameter declines the temperature and hence decreases the thermal boundary layer thickness when the shrinking sheet is prescribed with variable surface temperature. It is seen clearly that the dimensionless rate of heat transfer grows high as the values of Radiation parameter goes up.
- The effect of Heat generation parameter is to generate temperature for its increasing values. The dimensionless rate of heat transfer is reduced by increasing the value of Heat generation parameter. While the opposite trend is observed due to increase in Heat absorption parameter.
- The influence of Prandtl number is to reduce the temperature and the thermal boundary layer thickness. More amount of heat is transferred from the sheet to the fluid for increasing Prandtl number.
- All the profiles satisfy the far field boundary conditions asymptotically thus supporting the numerical results obtained.
- The study reveals that the reverse flow caused due to shrinking of the sheet can be controlled by applying a strong magnetic field. It is hoped that the present work will serve as a stimulus for needed experimental work on this problem.
- This study has potential applications in understanding the complex dynamics of many engineering and industrial flow systems. The interdisciplinary nature of boundary layer flow research presents a great opportunity for exploration and discovery at the frontiers of science and technology.

REFERENCE

[1]   Sakiadis, B. C., J. AIChe. **7** (1961) 26-28.
[2]   Sakiadis, B. C., J. AIChe. **7** (1961) 221-225.
[3]   Crane, L. J., Z Angew Math Physics **21** (1970) 645.
[4]   Chakrabarti, A., Gupta, A.S., Quart Appl Math. **37** (1979) 73-78.
[5]   Siddappa, B., Subhas, A., ZAMP **36** (1985) 890-892.
[6]   Dandapat, B. S., Gupta, A. S., Int. J. NonLinear Mech. **24** (1989) 215.
[7]   Elbashbeshy, E. M. A., Can. J. phys. **78** (2000) 1107-1112.
[8]   Liao, S.J., Int. J. Heat Mass Transf. **49** (2005)2529-2539.
[9]   Ishak, A., Nazar, R., Pop, I., Heat Mass Transfer **44** (2008) 921-927.
[10]   Prasad, K. V., Vajravelu, K., Datti, P. S., Int. J. NonLinear Mech. **45** (2010) 320-330.
[11]   Anjali Devi, S.P., Agneeshwari, M., Wilfred Samuel Raj, J., Int. J. of Applied Mechanics and Engineering **23** (2018) 289-305.
[12]   Miklavcic, M., Wang, C. Y., Quart. Appl. Mat. **64** (2006) 283-290.
[13]   Fang, T., Int. J. of Heat and Mass Transfer **51** (2008) 5838-5843.
[14]   Yao, B., Chen, J., Applied Mathematics and Computation **215** (2009) 1146-1153.
[15]   Fang, T., Zhang, J., Acta Mech. **209** (2010) 325-343.

[16]   Rohini, A. M., Ahmad, S., Ismail, A. I. Md., Pop, I., Int. J. of Thermal Sciences **64** (2013) 264-272.
[17]   Sajid, M., Javed, T., Hayat, M., Nonlinear dyn. **51** (2008) 259-265.
[18]   Fang, T., Zhang, J., Commu. Nonlinear Science and Num. Simulation **14** (2009) 2853-2857.
[19]   Noor, N.M.F., Hasim, I., Sains Malaysiana **38** (2009) 559-565.
[20]   Noor, N.M.F., Awang Kechil, S., Hasim, I., Commu. Nonlinear Science and Num. Simulation **15** (2010) 144-148.
[21]   Javed, T., Abbas, Z., Sajid, M., Ali, N., Int. J. of Heat and Mass Trans. **54** (2011) 2034-2042.
[22]   Lok, Y., Ishak, A., Pop, I., Sains Malaysiana **40** (2011) 1179-1186.
[23]   Bhattacharya, K., Chemical Engineering Research Bulletin **15** (2011) 12-17.
[24]   Suali, M., Nik Long, N.M.A., Ishak, A., App. Math. and Comp. Intel **1** (2012) 1-11.
[25]   Mahapatra, T. R., Sidui, S., Alexandria Engineering Journal **55** (2016) 163–168.
[26]   Bhatattacharya, K., Layek, G. C., Int. J. of Heat and Mass Trans. **15** (2011) 302-307.
[27]   Mahapatra, T. R., Nandy, S. K., Gupta, A. S., Meccanica **47** (2012) 1325-1335.
[28]   Nandy, S. K., Pop, I., Int. Commun. in Heat and Mass Trans. **53** (2014)50-55.
[29]   Anjali Devi, S. P., Wilfred Samuel Raj, J., J. of Applied Fluid Mech. **8** (2015) 613-621.
[30]   Yasin, M. H. M., Ishak, A., Pop, I., Journal of Magnetism and Magnetic Materials **407** (2016) 235-240.
[31]   Brewster, M. Q., Thermal radiative transfer properties, Wiley, Canada, (1992).
[32]   Raptis, A., Perdikis, C., Takhar, H. S., Applied Math. and Computation **153** (2004) 645-649.
[33]   Kandasamy, R. M., Khamis, A. B., Applied Math. And Mech. **29** (2008) 1309-1317.